Mechanical and Thermal Analysis of Performance of Compressed Earth Blocks with Sawdust Material Stabilized with Cement

Ryad Bouzouidja(✉), Tingting Vogt Wu, and Mehdi Sbartai

UMR CNRS 5295, Université de Bordeaux, 2M Bordeaux, Bordeaux, France
{ryad.bouzouidja,tingting.vogt-wu,mehdi.sbartai}@u-bordeaux.fr

Abstract. The aim of this study is to use local resources, namely raw earth and sawdust wood to be used in building materials, in order to contribute to solving the housing problem and to reduce the energy consumption, through the use of raw earth constructions. To achieve this objective, the mechanical, physical properties (Young's modulus, maximum compression stress, and flexural strength) and thermal properties (thermal conductivity and heat capacity) of raw earth bricks physically stabilized with cement (5%) and incorporating sawdust wood (3%; 5% and 10%) were studied. The results show that the sawdust-raw earth has interesting behavior with a maximum compressive strength of about 4 MPa. In addition, the results show that sawdust reduces the mechanical properties of earthen blocks but increases their ductility. The incorporation of 10% of sawdust decreases the Young's modulus of raw earth of 30% comparing to 3% of sawdust. In addition, the results showed that the thermal conductivity decreased from 1.1 W m^{-1} K^{-1} for the 3% sawdust sample, to 0.8 W m^{-1} K^{-1} for the 5% sawdust sample, and 0.7 W m^{-1} K^{-1} for the 10% sawdust sample, indicating an improvement in thermal insulation. Therefore, the results of this study give additional critical feedback to assist in evaluating the potential applications of sawdust as an insulating material for unfired clay blocks.

Keywords: Raw Earth Material · Thermal Conductivity · Compressive Strength

1 Introduction

The building sector is currently responsible for the world's greenhouse gas emissions and also almost 36% of global energy consumption (International Energy Agency, 2020). The most common material used in construction is concrete (mostly made by Portland cement). It represents more than 25 billion tons [1–3]. Concrete is widely used in various industries (e.g. construction of bridges, dams, buildings, tunnels and many physical infrastructures) [4, 5]. Large-scale consumption of concrete has strained natural sources of raw materials in recent decades [6]. It is therefore essential to identify solutions in order to reduce the energy demands of buildings without impacting the performance of the building and without altering its structure.

S. Amziane et al. (Eds.): ICBBM 2023, RILEM Bookseries 45, pp. 324–332, 2023.
https://doi.org/10.1007/978-3-031-33465-8_26

The use of concrete is today confronted with strong contradictions. The need in terms of cost and reduced carbon impact. However, identifying the carbon footprint of concrete remains complex. Purnel [7] reported that attributing a value for the quantity of carbon dioxide emitted per unit of production to the major structural materials is not straightforward. Considering that the majority of concrete is reinforced concrete. The carbon impact calculation includes contributions from cement, reinforcing steel, aggregates, water and admixtures. In general, the carbon impact is between 0.07 and 0.45 $kgCO_2\ kg^{-1}$ reinforced concrete [7]. Such increase in cement use will significantly increase the amount of CO_2 emissions in the atmosphere and cause global warming impacts [8]. The production of each ton of cement (e.g. Portland, clinker) releases an equivalent mass of CO_2 into the atmosphere. In reality, this amount released varies considerably depending on the energy efficiency of the plant and its age [9]. Different ways are suggested to minimize the use and the environmental impacts of concrete, namely, reduce, reuse, and recycle. Among these strategies, biosourced concrete is the most widely adopted strategy worldwide, partly due to its ease of implementation and the availability for the biosourced products, namely hemp, wood sawdust or raw earth. Considering only the manufacturing phase, Maskell et al. [10] founded that elying on the Inventory of Carbon and Energy (ICE) [11] and Ecoinvent [12] databases, that the choice of unfired extruded clay brick induces an embodied energy saving of 86% and of 25% as a reduction of 86% and 72% for CO_2 emissions in comparison, respectively, to fired clay and concrete blocks.

Raw earth materials such as brick have several environmental, social and economic benefits, their use contributes in minimizing the negative effects of the building on the environment while increasing energy savings [13]. The processing and handling of raw earth materials requires only 1% of the energy needed to manufacture and process the same volume of cement concrete [14]. Similarly, the manufacture of compressed earth blocks requires almost one third of the energy needed to manufacture conventional fired bricks, i.e. 440 kWh m^{-3} compared to 1300 kWh m^{-3} [15]. It is true that concrete allows the design of self-supporting walls, to have a low thermal inertia. However, one of the disadvantages of concrete is heat transfer. Concrete, being one of the most commonly used construction materials, its thermal conductivity draws importance [16]. For example, the thermal conductivities of concrete components (e.g. rocks) can vary from 1.163 to 8.6 W $m^{-1}K^{-1}$ [17].

The use of raw earth as a construction material can significantly reduce the environmental impact of current building practice. Raw earth can be locally sourced. In order to improve thermal and mechanical behavior of the raw earth material, two stabilization methods, i.e. chemical and physical, are actually applied [10]. The physical method consists of performing a granular correction and then incorporating fibers [18].

The aim of this study is to valorize local resources, namely earth and hemp to be used in building materials, in order to contribute to solving the housing problem and to reduce the energy consumption, through the use of raw earth constructions. To achieve this objective, it was decided to study the mechanical, physical and thermal properties of raw earth bricks physically stabilized with lime and incorporating hemp.

2 Materials and Methods

2.1 Materials

The local materials used are sand, clay and sawdust. The sand used was crushed sand with a particle size distribution of 0–4 mm from the Massif Central region in France according to the standard XP P13–901. The clay used in this study is an *illite* type provided by the CM Quartz Company. It is supplied from the same location as the sand. The sawdust material is a local product provided by the sawmill close to Bordeaux. This sawdust is produced by a chainsaw ref. TV3–15. The cement used in this study is a grey cement (grade 32.5) manufactured by Lafarge (65–79% of clinker).

The properties of the different martials are presented in Table 1.

Table 1. Physical characteristics of the used material. $^{\Delta}$, *, $^{+}$, $^{\blacklozenge}$ are defined as the different formulation (BTC0, BTC3, BTC5, and BTC10 respectively).

Material	Ratio (%)	Initial water content (wt%)	Density (kg m^{-3})
Sand	75^{Δ};72*; 70^{+}; $65^{\blacklozenge}$	0.6	620
Clay	20	3.1	670
Cement	5	29.9	370
Sawdust	0^{Δ};3*; 5^{+}; $10^{\blacklozenge}$	1.6	252

2.2 Sampling

The formulations were mixed using concrete mixer. The mortar preparation was made as follow. First, 30 wt% of sand and 70 wt% of clay were mixed together. Then, the water-saturated sawdust have been added gradually. After homogenization of the mixture using a vibrating table, the material was placed in the mold and compacted immediately. The parallelepiped (10 × 10 × 10 cm) and (23 × 5.6 × 5 cm) specimens were made by pressing using the hydraulic press of 3.7 MPa. The specimens were stored in plastic bags and after 28 days of curing, physical, mechanical, and thermal conductivity tests were performed.

To determine the particle size distribution, the sieving method was used. A sand specimen of about 200g was taken from the sand sample, it was then put in an oven to dry for 24 h. After the drying time, the sand was used to determine the particle size distribution using 14 sieves with different openings [19]. Also, a test for geometrical properties of aggregates – assessment of fines was done based on standard NF EN 933–8. The objective of this test is to rapidly assess the relative portion of clay in the sand that is to be used in construction. A low value of sand equivalent describes the fine aggregate as “dirty” and indicates that possibly the clay materials are harmful.

2.3 Thermal and Mechanical Experiments

In this part of the work, the thermal characterization method was used for the measurement of thermal conductivity λ [W m^{-1} K^{-1}] and volumetric heat ρc [J K^{-1} m^{-3}]. These properties were assessed in accordance with Standard ISO8301 [20] and NF 12667 [21]. These methods are based on a steady state technique. The measurements were made using a heat flux probe (accuracy ± 20W m^{-2}) and type T thermocouple (accuracy ± 1.0 °C). The sample is placed between two exchanger plates (see Fig. 1).

To determine thermal conductivity the method consists in in subjecting a sample of thickness l to a temperature gradient, of so as to impose a flow transfer from the hot side to the cold side. The exchanger plates are maintained at different temperatures (θ_1 and θ_2, expressed in °C). It is important to note that when studying wet porous materials, the stresses thermal conditions imposed on the system can cause mass transfers to appear during the handling. In this type of material, it is necessary to impose a limited temperature difference to avoid coupled transfers.

Volumteric heat capacity is determined using the same measurement as the thermal conductivity, only imposed thermal stresses change. The sample-flowmeter system is first subjected to the stabilized temperatures of the exchanger plates until an equilibrium state is reached. It is then made to evolve towards another state of equilibrium by changing one or more instructions of the thermostatic baths.

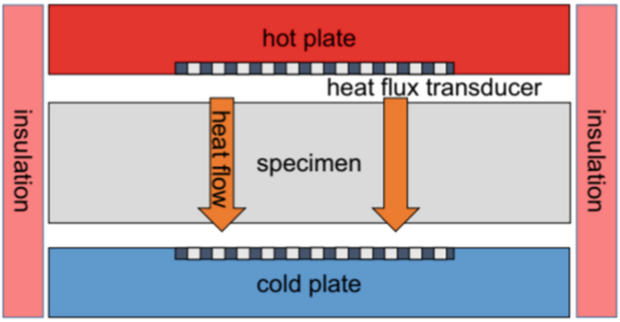

Fig. 1. Schematic diagram of the principle of the heat flow meter based on Kim et al. study [22].

Compressive strength was carried out on cubic blocks (10 × 10 × 10 cm) using hydraulic press. The sample compression test was carried out using a Picsx with a capacity of 100 kN with a loading speed of 0.5 mm min^{-1} and Testwork software. The specimens were equipped with three Linear Variable Differential Transformer (LVDT) sensors to measure the longitudinal deformation [23] (Fig. 2).

Three-point bending tests were also performed on beams of dimension. The tests were performed according to RILEM-TMC 50 recommendations on beams at 28 days of age and kept in a climatic room at 20 °C and 60% RH. Bending tests were performed using an electromechanical machine with a capacity of 100 kN. Unnotched beams were used to avoid stress concentrations at early age that can cause early beam failure. The test was driven with a CMOD (Crack Mouth Opening Displacement) notch opening

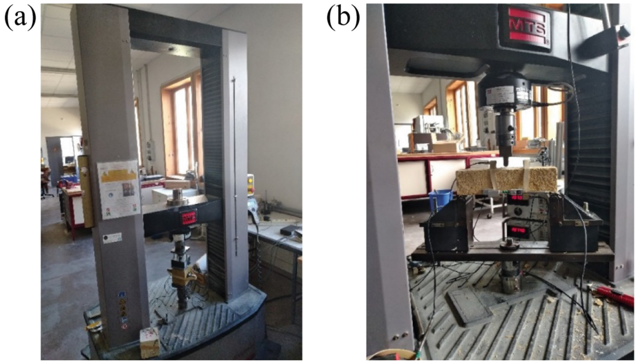

Fig. 2. Compressive test device used for (a) compressive strength and (b) three-point bending test.

system with two LVDT sensors (0.01 μm accuracy) placed on both faces of the beam at the bottom center.

These two sensors were placed on the beam by two metal supports glued to the specimen. The aluminum plates, supports for the LVDT sensors, were glued at a distance equivalent to half the height from the middle of the beam to ensure that the crack appears between these two plates. Although this measurement is not exactly the CMOD in the case of unbraced beams, for simplicity it has been called as such. The crack opening velocity was varied during the test with a velocity of 0.05 mm min^{-1} before the peak and a velocity of 0.4 mm min^{-1} towards the end to accelerate the failure in the stable softening phase. The deflection was also measured in the middle with an LVDT sensor and a measurement system to avoid problems related to concrete crushing at the supports.

3 Results and Discussion

3.1 Physical and Mechanical Properties

Figure 3 presents the grain size distribution of the sand. From this figure, the curve shows a regular distribution of particle size and favoring a specific range of diameter greater than or equal to 0.8 mm, which represents 60% in mass proportion. The fine sieved fraction which corresponds to the clayey texture represents a proportion of 4.8%. The clay fraction represents 1.2%. Sand equivalent (SE) test is around 65%. According to the French specifications ($60 < SE < 70$) is sand is suitable for use in building construction, cleanliness for quality concrete not particularly afraid of shrinkage.

Table 2 shows the results of the compressive strength and Young's Modulus. According to the results, we note that the stress evolves proportionally linearly with the deformation. This evolution verifies Hook's law. In this part the sample has an elastic behavior.

The slope of the linear regression line is called Young's modulus and its value is 10.9 GPa. After 0.0005 deformation, the stress changes with the deformation until it reaches a maximum value of 17.3 MPa before collapsing completely: This is the compressive strength. It turns out that the characterized material has a ductile behavior. It will thus

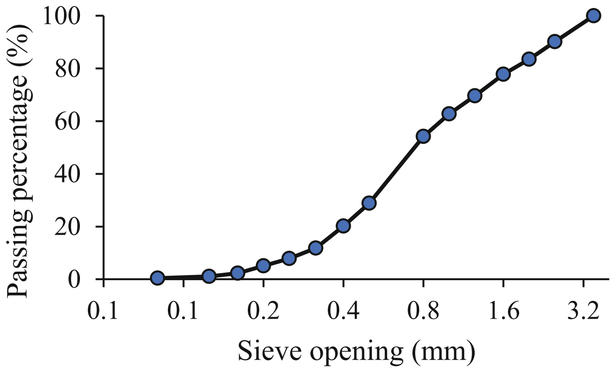

Fig. 3. Granulometery of the sand sample.

Table 2. Compressive stress and young modulus of wood sawdust reinforced concrete.

Ref	Density (kg m^{-3})	Compressive strength (N mm^{-2})	Flexural strength (MPa)	Young's Modulus (GPa)
BTC3	1697.2 ± 55.0	2.4 ± 0.4	0.7 ± 0.1	3.0 ± 0.3
BTC5	1697.3 ± 6.3	2.7 ± 0.3	0.6 ± 0.1	2.2 ± 0.4
BTC10	1624.9 ± 2.4	1.9 ± 0.4	0.4 ± 0.1	1.0 ± 0.2
BTC0	1936.3 ± 1.2	17.3 ± 0.5	2.1 ± 0.1	10.9 ± 0.7

be able to work in compression and withstand very large loads. It could, for example, be used in the construction of load-bearing walls, partitions, carry frames. It noted also a decrease of density of the reference (BTC0) 1936 kg m^{-3} to around 1600–1700 kg m^{-3} (BTC3, BTC5 and BTC10) by raising the treated fibers percentage. The same observation is made for the bending behavior. The reduction in compressive strength could be caused by non-uniform dispersion or segregation of fibers in the earth's matrix [23].

3.2 Thermal Properties

Figure 4 shows the results of a thermal conductivity and density for the different prepared samples. The results show that the thermal conductivity decreases with adding sawdust and reducing sand to the clayey soil.

Sample BTC0 exhibits a conductivity of about 1.201 ± 0.031 W m^{-1} K^{-1}, and after adding 3% of sawdust (BTC3) this value slightly decreases to 1.167 ± 0.046 W m^{-1} K^{-1}. Then by adding 5% of sawdust the value of the thermal conductivity reaches 0.853 ± 0.004 W m^{-1} K^{-1}. This decrease is due to the modification of clay granularity by the reduction of sand in the mixture. Otherwise, the samples with 10% of sawdust (BTC10) exhibit the lowest thermal conductivity (0.766 ± 0.041 W m^{-1} K^{-1}).

This is due to both the incorporation of fibers into the clay matrix and the improvement of their adhesion to the earth matrix. This behavior is in consistency with several authors' results [24] who had observed the decrease in thermal conductivity with the increase in the percentage of fibers.

Figure 5 shows the results of the volumetric specific heat (VSH) of raw earth bricks stabilized with sawdust contents. It was noted that when the sawdust content went from 0% to 10%, the VSH decreases from 2060.6 kJ m $^{-3}$ K^{-1} to 1821.3 kJ m $^{-3}$ K^{-1}.

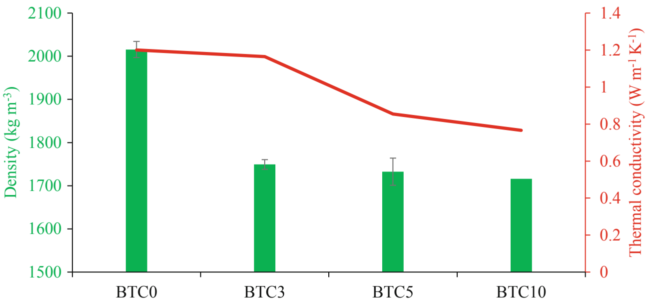

Fig. 4. Density (green bars) and thermal conductivity (red bars) of raw earth materials reinforced with sawdust. BTC0 means that no sawdust is added. BTC3 means that 3% of sawdust is added. BTC5 means that 5% of sawdust is used and BTC10 means that 10% of sawdust is used.

This can be explained by the fact that the incorporation of this fiber whose specific heat (wood family) is higher than that of the control clay block containing sand only.

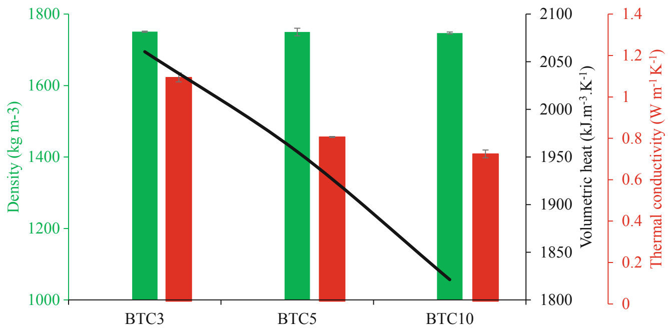

Fig. 5. Density (green bars), thermal conductivity (red bars) and volumetric heat (black continuous line) of raw earth materials reinforced with sawdust. BTC3 means that 3% of sawdust is added. BTC5 means that 5% of sawdust is used and BTC10 means that 10% of sawdust is used.

4 Conclusion

In this paper, the mechanical and thermal properties of cement-stabilized and sawdust-stabilized compressed earth bricks are investigated by experiments, and the relationships between the properties and factors are revealed. The experimental results show that the compressive properties of sawdust cement-stabilized compressed earth bricks are negatively correlated with the percentage of fiber addition. The thermal conductivity and specific heat of the compressed mud brick are positively correlated with the ratio of added sawdust. In this study, we test only the compressive strength, thermal conductivity and specific heat of the main structure. In the future, other indices of mechanical, durability or thermal properties may be added. This information may allow us to improve the understanding of the behavior of this type of material. Also, wall scale tests will be carried out.

References

1. Afroughsabet, V., Biolzi, L., Monteiro, P.J.M.: The effect of steel and polypropylene fibers on the chloride diffusivity and drying shrinkage of high-strength concrete. Compos. Part B Eng. **139**, 84–96 (2018). https://doi.org/10.1016/j.compositesb.2017.11.047
2. Celik, K., Meral, C., Mancio, M., et al.: A comparative study of self-consolidating concretes incorporating high-volume natural pozzolan or high-volume fly ash. Constr Build. Mater. **67**, 14–19 (2014). https://doi.org/10.1016/j.conbuildmat.2013.11.065
3. Cristino, T.M., Lotufo, F.A., Delinchant, B., et al.: A comprehensive review of obstacles and drivers to building energy-saving technologies and their association with research themes, types of buildings, and geographic regions. Renew. Sustain. Energy Rev. **135**, 110191 (2021). https://doi.org/10.1016/j.rser.2020.110191
4. McGinnis, M.J., Davis, M., de la Rosa, A., et al.: Strength and stiffness of concrete with recycled concrete aggregates. Constr. Build. Mater. **154**, 258–269 (2017). https://doi.org/10.1016/j.conbuildmat.2017.07.015
5. Yang, S.T., Li, K.F., Li, C.Q.: Numerical determination of concrete crack width for corrosion-affected concrete structures. Comput. Struct. **207**, 75–82 (2018). https://doi.org/10.1016/j.compstruc.2017.07.016
6. Tiwari, A., Singh, S., Nagar, R.: Feasibility assessment for partial replacement of fine aggregate to attain cleaner production perspective in concrete: a review. J. Clean. Prod. **135**, 490–507 (2016). https://doi.org/10.1016/j.jclepro.2016.06.130
7. Purnell, P.: The carbon footprint of reinforced concrete. Adv. Cem. Res. **25**, 362–368 (2013). https://doi.org/10.1680/adcr.13.00013
8. Nath, P., Sarker, P.K., Biswas, W.K.: Effect of fly ash on the service life, carbon footprint and embodied energy of high strength concrete in the marine environment. Energy Build. **158**, 1694–1702 (2018). https://doi.org/10.1016/j.enbuild.2017.12.011
9. Thomas, M., Barcelo, L., Blair, B., et al.: Lowering the carbon footprint of concrete by reducing clinker content of cement. Transp. Res. Rec. **2290**, 99–104 (2012). https://doi.org/10.3141/2290-13
10. Maskell, D., Heath, A., Walker, P.: Comparing the environmental impact of stabilisers for unfired earth construction. Key Eng. Mater. **600**, 132–143 (2014). https://doi.org/10.4028/www.scientific.net/KEM.600.132
11. Hammond, G., Jones, C.: Inventory of carbon & energy: ICE. Sustainable Energy Research Team, Department of Mechanical Engineering (2008)
12. Hischier, R., Weidema, B., Althaus, H., et al.: Implementation of life cycle impact assessment methods. Ecoinvent report no. 3, v2. 2 (2010)
13. Pittet, D., Jagadish, K.S., Kotak, T., et al.: Environmental impacts of building technologies: a comparative study in Kutch District, Gujarat State, India. In: Bolay, J.-C., Schmid, M., Tejada, G., Hazboun, E. (eds.) Technologies and Innovations for Development: Scientific Cooperation for a Sustainable Future, pp. 113–128. Springer, Paris (2012). https://doi.org/10.1007/978-2-8178-0268-8_9

14. Deboucha, S., Hashim, R.: A review on bricks and stabilized compressed earth blocks. Sci. Res. Essays **6**, 499–506 (2011). https://doi.org/10.5897/SRE09.356
15. Little, B., Morton, T.: Building with earth in Scotland: Innovative design and sustainability. Scottish Executive Central Research Unit Edinburgh (2001)
16. Khan, M.I.: Factors affecting the thermal properties of concrete and applicability of its prediction models. Build. Environ. **37**, 607–614 (2002). https://doi.org/10.1016/S0360-1323(01)00061-0
17. Asadi, I., Shafigh, P., Abu Hassan, Z.F.B., Mahyuddin, N.B.: Thermal conductivity of concrete – a review. J. Build. Eng. **20**, 81–93 (2018). https://doi.org/10.1016/j.jobe.2018.07.002
18. Losini, A.E., Grillet, A.C., Bellotto, M., et al.: Natural additives and biopolymers for raw earth construction stabilization – a review. Constr. Build. Mater. **304**, 124507 (2021). https://doi.org/10.1016/j.conbuildmat.2021.124507
19. Dishman, K.L.: Sieving in particle size analysis. In: Encyclopedia of Analytical Chemistry. John Wiley & Sons, Ltd. (2006)
20. ISO 8301 (1991). https://viewerbdc.afnor.org/Pdf/Viewer/AXlEBc-V7yA1. Accessed 1 June 2021
21. NF EN 12667 (2001). https://viewerbdc.afnor.org/Pdf/Viewer/C4G_g4acsMA1. Accessed 1 June 2021
22. Kim, D., Lee, S., Yang, I.: Verification of thermal conductivity measurements using guarded hot plate and heat flow meter methods. J. Korean Phys. Soc. **78**(12), 1196–1202 (2021). https://doi.org/10.1007/s40042-021-00177-0
23. Shiming, S., Yupu, S.: Dynamic biaxial tensile–compressive strength and failure criterion of plain concrete. Constr. Build. Mater. **40**, 322–329 (2013). https://doi.org/10.1016/j.conbuildmat.2012.11.012
24. Laborel-Préneron, A., Magniont, C., Aubert, J.-E.: Hygrothermal properties of unfired earth bricks: effect of barley straw, hemp shiv and corn cob addition. Energy Build. **178**, 265–278 (2018). https://doi.org/10.1016/j.enbuild.2018.08.021